

<https://doi.org/10.1038/s44264-026-00134-z>

Non-targeted root exudome profiling reveals genotype-specific strategies for phosphorus use from conventional and recycled sources



Michael Walsh^{1,2}, Philippe Schmitt-Kopplin^{3,4}, Jenny Uhl³, Marianna Lucio³, Hector Vera Wood¹, Gerhard Schenk⁵, David Jordan⁶, Emma Mace⁶ & Susanne Schmidt¹ ✉

Phosphorus use efficiency (PUE) is a vital crop trait encompassing both acquisition and internal utilisation efficiencies. To address knowledge gaps in crop PUE and the growing application of phosphorus (P) recycles, we investigated early growth and root exudation in sorghum genotypes. We tested the hypothesis that P-efficient landraces (SC283-14E and SC648-14E) outperform an inbred line (BTx623, bred under high-P conditions, with unknown PUE status) when supplied with less soluble P sources. Four P sources were applied, ranging from low to high solubility: rock phosphate (RP) < P recycle hazenite (Haz) < single superphosphate (SSP) < mineral solution (MS). After 28 days of growth under low P supply, root exudates (125–2000 amu) were comprehensively profiled using FT-ICR-MS. Biomass production and P accumulation varied significantly among genotypes and P sources, with notable genotype × P source interactions. Compared to BTx623, SC283-14E produced greater root biomass with RP and higher total biomass with SSP, and accumulated more P with MS than the other genotypes. Genotype-specific exudates were identified across all P sources: phaseic acid (SC283-14E), flavonoids and/or polyphenols (SC648-14E), and amino acids and/or amino sugars (BTx623). Hazenite elicited the most distinct exudome profiles: SC283-14E released flavonoid dimers, tannins, and phenolic acid derivatives; SC648-14E exuded putative phenolic dimers and/or flavonoids; and BTx623 produced sulphur- and nitrogen-containing conjugates, including sulphonated peptides and amino acids. These findings highlight the potential of leveraging root exudate profiles in crop breeding for enhanced PUE in the circular phosphorus economy that recovers nutrients from agricultural, industrial, and food waste streams.

Root exudates play a critical role in nutrient acquisition, either by directly mobilising nutrients from the growth medium or indirectly acquiring nutrients through microbial actions^{1,2}. However, root exudates are under-exploited in the quest to breed nutrient-use-efficient crops, not least due to a limited understanding of the exudates of wild crop relatives and landraces that are a large potential source of information and genetic material for modern breeding programmes^{3,4}. In the context of phosphorus use

efficiency (PUE), low-molecular-weight exudates such as organic acids and phytosiderophores or enzymes (e.g., phosphatases) have been widely studied⁵. However, many exudates remain unidentified, and the emerging field of exudomics is addressing this gap through advanced technologies, including non-target Fourier Transform Ion Cyclotron Resonance Mass Spectrometry (FT-ICR-MS) to connect exudomic data with genomics, offering valuable insights for crop breeders^{6,7}. Root exudates are relevant for

¹School of Agriculture and Food Sustainability, The University of Queensland, Brisbane, QLD, Australia. ²End Food Waste Cooperative Research Centre, Wine Innovation Central Building, Waite Campus, Adelaide, SA, Australia. ³Research Unit Analytical BioGeoChemistry, Helmholtz Munich, Neuherberg, Germany. ⁴Chair of Analytical Food Chemistry, Technical University of Munich, Freising, Germany. ⁵School of Chemistry and Molecular Biosciences, The University of Queensland, Brisbane, QLD, Australia. ⁶Queensland Alliance for Agriculture and Food Innovation, The University of Queensland, Brisbane, QLD, Australia.

✉ e-mail: Susanne.Schmidt@uq.edu.au

the emerging circular nutrient economy that repurposes fertiliser nutrients from waste streams, with efficiency gains expected by aligning genotypes with next-generation fertilisers for target pedoclimatic conditions and agronomies. Thus, root exudome analysis can support the transition towards nutrient use efficiency, expanding 'omics tools.

Next-generation fertilisers are gaining momentum as they reduce a region's or nation's dependence on conventional P fertilisers. Most currently used mineral P fertiliser are mined from non-renewable mineral deposits at great environmental cost, are subject to price volatility and supply chain uncertainties with mineral P deposits restricted to a few regions globally, and are often inefficient, with only half the applied P fertiliser incorporated by global crops⁸. Leveraging knowledge of root exudates has the potential to advance use of a broad range of P sources, including sewage ash, struvite, hazenite, and organic materials—such as manures and composts from food wastes—as viable alternatives to conventional P fertilisers^{9–11}. Recycled P sources such as sewage ash and struvite can supply crops when paired with suitable crops and growth environments^{10,12}, with the circular P economy enabled by consortia of engineers, fertiliser designers, crop breeders and agronomists.

Numerous crop traits determine P efficiency. Internal PUE refers to the plant's ability to use acquired P efficiently through metabolic adjustments in response to P limitation, including remobilising P from source to sink tissues^{13,14}. External PUE is the efficient acquisition of P from the growth medium, which is facilitated by root architecture, mycorrhizal associations, microbial interactions and root exudates, for example, carboxylates and enzymes that mobilise P from inorganic and organic sources, respectively^{15,16}. Phosphorus sources such as rock phosphate and some recycles have low solubility, which can limit their effectiveness as fertilisers. For example, rock phosphate¹⁷, sewage ash (AshDec®, Raniro et al.¹⁰) and struvite¹⁸ can exhibit low relative fertiliser efficiency compared to more readily water-soluble commercial fertilisers such as triple superphosphate. However, when paired appropriately with target crops and environments, low-solubility P sources can perform as well as, or even outperform, conventional fertilisers^{10,18,19}. Since fertiliser effectiveness depends on complex interactions between crop genotype, P source and environment, it is essential to understand the causalities.

We used FT-ICR-MS non-target analysis to develop exudomics as a tool to improve the PUE of sorghum. Sorghum was chosen as a versatile, climate-resilient crop used for (gluten-free) food, livestock feed, as biofuel and biomaterial production²⁰. Genetic improvement of sorghum is well advanced, as sequencing of numerous genotypes has revealed a large pool of genetic diversity and domestication history linked to functional traits²¹.

Root exudates, including phenolics, flavonoids and others, can promote microbial activity, including P-solubilizing bacteria, and can have allelopathic effects, as seen with ferulic acid²² and sorgoleone^{23,24}. Sorghum-specific sorgoleone promoted root colonisation by arbuscular mycorrhizal fungi^{25,26}, and the increased phenolic exudation of sorghum mutant BTx623 enriched beneficial rhizosphere bacterial communities²³. To isolate the direct effects of exudates on P mobilisation, our study minimised microbial interactions in controlled experimentation.

Here, we explored root exudation as a tool for breeding PUE sorghum. We compared two landraces and one improved inbred line, hypothesising that the landraces, having been selected in lower P environments than the inbred line, outperform the inbred line under conditions of low P availability. Analysis of growth, P acquisition and root exudates using P sources of different solubility and lines with contrasting genetic backgrounds has the potential to advance understanding of how sorghum modulates exudate profiles.

Methods

Seed preparation and germination

We selected three *Sorghum bicolor* (L.) Moench lines from a previously characterised diversity panel, predominantly consisting of genotypes from the Sorghum Conversion Program²⁷. The genotypes included (i) SC283-14E a converted landrace from Tanzania (mixed race) characterised by high root

surface area that was positively correlated with PUE under low P conditions²⁸, (ii) SC648-14E a converted landrace from South Africa (kafir) characterised by its relationship with arbuscular mycorrhizal fungi and high P uptake capacity²⁹, and (iii) BTx623 (PI 659985 MAP) a widely used inbred line (mixed race) developed under high-input agricultural conditions, serving as the reference genome for sorghum and exhibiting extensive variations^{30,31}. Seeds were sterilised with a solution containing 100 ml bleach, 100 ml autoclaved milli-Q water, and 50 μ l Tween 20 detergent³² and suspended in the sterilisation solution for 1.5 h using a rotary rube mixer (Ratek, RSM7DC) at 1.5 rotations per minute. Seeds were taken to a sterilised laminar flow cabinet where the sterilisation solution was removed via pipette. The seeds were rinsed with autoclaved Milli-Q water and lightly suspended before being removed via pipette. The rinsing step was repeated 6 more times. Seeds were then placed into Petri dishes with filter paper (Whatman®, 1001-085) moistened with autoclaved milli-Q water and positioned in a sterilised growth cabinet and semi-uncovered. Germinates were transferred into the microcosms (see below) upon radicle emergence.

Experimental details: growth medium, microcosms and fertiliser

The growth medium comprised of a 1:1 (v/v) mix of fine-grain silicate sand (crystalline silica, Richgro washed play sand) and coarse river sand (washed Brisbane River sand provided by the University of Queensland glasshouse services) to ensure a fine but sufficiently porous substrate. The sand was washed with Decon 90, a P-free surfactant, followed by repeated rinsing with autoclaved milli-Q water. Potassium chloride was used to neutralise the growth medium to a final pH of 6.85 and placed in an oven at 110 °C to dry for 48 h³³. The microcosm design was a modified 50 mL Falcon Tube³⁴ with an open top and base of 27 and 21 mm diameter, respectively. The base was inset with two layers, which included a 0.2 mm thick stainless steel mesh underlying glass microfibre filter paper (Whatman®, GF/A). Microcosms were filled with 40 g of sand, followed by fertiliser deposited 2.5 cm below the surface, and filled with an additional 35 g of sand and placed in an oven at 62.5 °C for 72 h.

Phosphorus sources included granules with 1.5 \pm 0.1 mm diameter (rock phosphate (RP), hazenite (Haz), and single superphosphate (SSP)). Each microcosm received 5 mg P at the start of the experiment (except the mineral solution control, see below). Selected fertiliser pellets were placed in the oven at 62.5 °C for 48 h followed by UV exposure for 30 min for sterilisation. The control plants received mineral solution (MS) with an initial 0.1 mL 91.4 mM KH₂PO₄ and 8.5 mM K₂HPO₄ in the first week, which incrementally increased to 0.25, 0.5 and 1.0 mL after each consecutive week (totalling 20 mg P at the end of the 4-week experiment). All treatments received a complete (no added P) nutrient solution every second day, with 1 mL nitrogen solution containing NH₄NO₃ initially at 2.5 mM and incrementally increasing to 5, 10 and 20 mM each consecutive week. All other nutrients were provided as solution with 1 mM K₂SO₄, 1 mM MgSO₄, 1 mM CaCl₂, 200 μ M FeEDTA, 10 μ M MnSO₄, 10 μ M H₃BO₃, 1 μ M CuSO₄, 3 μ M ZnSO₄ and 0.35 μ M Na₂MoO₄.

Treatments were arranged in a randomised block design. Plants were grown in a growth cabinet (NVIRON, A1000) for 28 days post-planting and received full-spectrum artificial light for 18 h at 30 °C, and no light for 6 h at 28 °C. Photosynthetic photon flux density in the growth cabinet equalled 200 for the first 14 days, and 480 for the remaining 14 days (PPF-UV = 2.28, PPF-B = 98.71, PPF-G = 189.97, PPF-R = 192.42, PPF-NIR = 20.33). Correlated colour temperature, lux and absorption peak equalled 4689 K, 29871 lm m² and 660 nm, respectively. Water holding capacity (WHC) of the microcosms was calculated daily by weighing each tube and maintained at 90%. The microcosm surface was lightly sprayed with autoclaved milli-Q at mid-day and late afternoon to avoid drying out. Microcosms were flushed at the end of weeks 1, 2 and 3 at 200% WHC to mitigate potential salinity.

Exudate collection and FT-ICR-MS analysis

On day 28, the leachate was collected within the same light and temperature conditions between 10:00 and 16:00 to minimise diurnal effects³⁵. Autoclaved milli-Q water was used to flush 150% WHC, and 2 \times 1.5 mL of

leachate was collected in 2 mL Thermo Scientific™ Screw Cap Micro Tubes with an altered pierced cap for air-transfer sublimation during the freeze-drying step. Samples caps were covered with parafilm and immediately transferred to a -80°C freezer for 72 h. The parafilm was then removed from the sample caps and placed in a freeze dryer (VirTis®, BenchTop Pro with Omnitronics™) at 71 mT, -48.5°C , for 48 h.

Freeze-dried exudate samples were rehydrated using 400 μL milli-Q water and vortexed until solubilised. Sample pH was adjusted to 2 using 0.5 μL HCl (32%). A further 50 μL of methanol was leached through an OMIX C18 100 μL tip, followed by 100 μL of acidified water (pH 1.5). The exudate solution was leached through a C18 tip, followed by 100 μL of acidified water. Lastly, 50 μL of methanol was flushed through the C18 for analysis. Samples were loaded and analysed by the FT-ICR-MS at a pump injection rate of 2 $\mu\text{L min}^{-1}$ (methanol).

We chose non-target analysis to detect biochemicals in the range of molecular masses of 125–2000 amu. Samples were analysed on a high-field FT-ICR-MS from Bruker Daltonics with a 12-T magnet from Magnex. A time domain transient with four million data points (4 MWords), representing the recorded signal from ion oscillations in the magnetic field, was obtained and Fourier-transformed into a frequency domain spectrum. The frequency domain was afterward converted to a mass spectrum by the SolariX Control program of Bruker Daltonics. The ion excitations were generated in broadband mode (frequency sweep radial ion excitation), and 500 scans were accumulated for each mass spectrum in a mass range of 120–1000 amu. Ions were accumulated for 300 ms before ICR ion detection. The pressure in the quadrupole/hexapole and ICR vacuum chamber was 3×10^{-6} mbar and 6×10^{-10} mbar, respectively.

Data were analysed using the software Bruker Compass DataAnalysis 5.0 SR1 (x64) version 203.2.3586, with a smooth width (m/z) of 0.0002 (Da) with 10 cycles. Internal calibration search ranges from 0.005 (m/z) ± 0.2 ppm. FT-ICR-MS with m/z from 120 to 1000 amu were calibrated externally and internally to preclude alignment errors. Subsequently, the mass spectra were exported to peak lists at a signal-to-noise ratio ≥ 3 . Elemental formulas were calculated combinatorially within a mass accuracy window of ± 0.2 ppm for each peak in batch mode by an in-house software tool and validated via the senior-rule approach/cyclomatic number, assuming valence 2 for sulphur (S).

FT-ICR-MS analysis enables highly resolved ($R > 106$ at m/z 200) and accurate chemical mass analysis of electrospray-generated ions within a 200 ppb error window over a wide mass range from m/z 100 to 1000. The weight of the ions is measured with a precision lower than the mass of an electron ($\Delta m/z = 0.0003$ amu), and the specific signals can be differentiated with the same mass precision due to the ultrahigh resolution. These exact masses of the ions can routinely be converted into unique compositional formula bearing the light elements carbon (C), hydrogen (H), nitrogen (N), oxygen (O), and S (or any other element in the target), also taking account of their possible chloride and sodium adducts and of their natural isotopic abundance. The solvent extracts generated over 20,000 thousands of individual signals that were converted into elementary compositions (elemental family) and represented in van Krevelen type of diagrams (H/C vs. O/C) or related (H/C vs m/z) in which each formula is represented by a dot (the size of the dot is proportional to its abundance) as a projection of the relative oxygenation degree (O/C) and saturation degree (H/C) for various classes of compound types (CHO, CHNO, CHOS, CHNOS). Analysed compounds were limited to a maximum of four N and P metabolites were excluded from the analysis.

Biomass and root length analysis

After leachate collection, above-ground biomass was harvested and placed into an oven at 39°C for 72 h. The growth medium was washed, and roots removed by rinsing with deionised water. Roots were placed on a transparent plastic dish and scanned to quantify root characteristics (Epson Expression 10000XL, B11B168031) at 16-bit Greyscale with 800 dpi resolution. Scanned root images were prepared using Adobe Photoshop (version 24.7.4) to remove residual growth medium and background incidentals.

Scanned root images were analysed using WinRHIZO™ software (version 2019a) with 15 root classes with 0.1 mm intervals (<0.1 to >1.4 mm). After scanning was completed, roots were dried at 39°C for 72 h in an oven. Shoot and root dry weight was recorded before ICPOES analysis (5% nitric acid digestion, Thermo iCAP PRO XP) to quantify total P.

Statistical analyses and graphical representations

To analyse the measured plant traits across genotypes and P treatments, we performed a two-way analysis of variance (ANOVA) for total biomass dry weight, shoot and root biomass, total root length, and total plant P content, followed by a Tukey test for post hoc multiple comparisons at a significance level of $p \leq 0.05$. Principal component analysis (PCA) and partial least squares-discriminant analysis (PLS-DA) were conducted using R statistical software to investigate the clustering and separation of samples based on their chemical compositions. Confidence ellipses were calculated based on a 95% confidence interval to illustrate the distribution of the samples within each group. Both analyses were performed with 'mixOmics' and 'ggplot2' packages in R. A hierarchical cluster analysis (Hierarchical Clustering Explorer Version 3.5) allowed group samples based on their similarities across the dataset, where the dendrogram illustrates the relationships between treatments and respective genotypes by successively merging clusters according to their proximity in feature space.

Results

Plant growth and phosphorus acquisition

The effect of sorghum genotypes and P treatment (No P, rock phosphate RP, single superphosphate SSP, hazenite Haz, mineral solution MS) were analysed with the response variables of P acquisition, total biomass, shoot and root allocation, and root length (Fig. 1, Supplementary Table 1). The two-way ANOVA revealed a significant interaction ($F_{8, 45}$, 2.60, $p \leq 0.05$) between genotype ($F_{2, 45}$, 28.3, $p \leq 0.05$) and P treatment ($F_{4, 45}$, 251.9, $p \leq 0.05$). Similarly, comparing shoot and root weight, a significant interaction ($F_{8, 45}$, 4.22, $p \leq 0.05$ and $F_{8, 45}$, 3.28, $p \leq 0.05$, respectively) occurred between genotypes ($F_{2, 45}$, 14.5, $p \leq 0.05$ and $F_{2, 45}$, 29.0, $p \leq 0.05$, respectively) and P treatment ($F_{4, 45}$, 432, $p \leq 0.05$ and $F_{4, 45}$, 101.7, $p \leq 0.05$, respectively). Two-way ANOVA determined no significant interaction ($F_{8, 45}$, 0.879, $p = 0.541$) between genotype and P treatment on total root length, with differences between genotype ($F_{2, 45}$, 12.1, $p \leq 0.05$) and P treatment ($F_{4, 45}$, 12.4, $p \leq 0.05$). Total root length was largely consistent across all genotypes and treatments, except for SC283-14E and SSP, Haz, and MS treatments, which exceeded the SC648-14E and BTx623 No P and RP treatments.

Plant P content showed significant interactions ($F_{8, 45}$, 3.07, $p \leq 0.05$) between sorghum genotypes ($F_{2, 45}$, 4.61, $p \leq 0.05$) and treatments ($F_{4, 45}$, 1430, $p \leq 0.05$). The total P content was approximately four-times greater in the MS control and Haz treatments, consistent with the four-times higher P supply with MS compared to the other P treatments (20 and 5 mg P microcosm $^{-1}$, respectively). No P control, RP, and SSP treatments had mostly similar P contents.

MS treatments had significantly more shoot biomass than the other treatments, except BTx623, which matched Haz. Root and shoot biomass of No P and RP treatments were consistently lower than all other treatments, and root biomass of SC283-14E grown with RP, SSP and MS was significantly ($p \leq 0.05$) higher than BTx623 biomass.

Exudome—similarities and clustering analysis

Leachates were analysed with FT-ICR-MS to examine root exudate profiles (Fig. 2). A principal component analysis (PCA, Fig. 2a) and partial least squares discriminant analysis (PLS-DA, Fig. 2b) were conducted to identify P treatment clusters against plant responses denoted by the detected compounds. PC 1 and PC 2 (respectively) scores for the PCA and PLS-DA account for 11.2% and 7.1%, and 10.4% and 4.4%, respectively, of the total variance. The PCA illustrates that RP and MS treatments cluster separately from the other groups, while the remaining treatments have less distinct clusters. The clustering patterns in the PLS-DA reflect greater distinctions

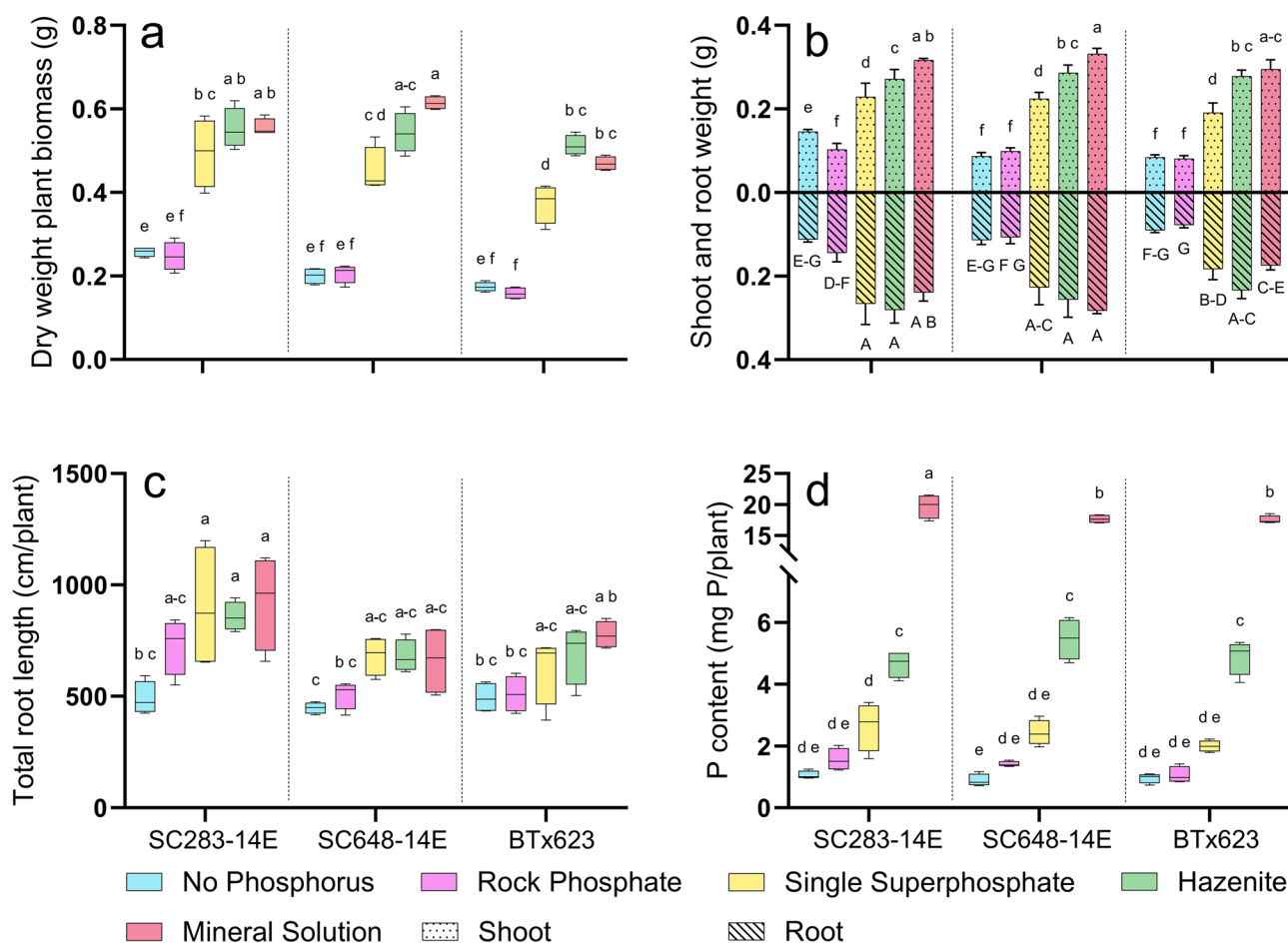


Fig. 1 | The effect of sorghum genotypes and P treatment (No P, rock phosphate RP, single superphosphate SSP, hazenite Haz, mineral solution MS). Biomass and phosphorus content of sorghum genotypes SC283-14E, SC648-14E and BTx623 ($n = 4$): a dry weight biomass (g plant^{-1}), b shoot and root dry weight (g plant^{-1}), c total root

length (cm plant^{-1}), and d total P accumulated biomass (mg P plant^{-1}). Data was analysed with two-way ANOVA and post-hoc Tukey test. Superscript letters represent significant ($p \leq 0.05$) differences between treatments. Error bars represent standard deviation. See Supplementary Table 1 for a detailed statistical analysis.

between treatments, and similar to the PCA, the MS treatment separates from the other treatments.

The van Krevelen diagram (Fig. 2c) shows 5240 detected compounds with elemental composition, summarised in the donut chart, with the distribution centred on CHO and CHNO compounds. The cluster of compounds and compound families with high signal intensity between 1.25–2.0 H/C and 0.2–0.5 O/C indicate a diverse presence of compounds, including, but not limited to, low molecular weight organic acids, polyketides, polyphenols, flavonoids, terpenoids, lipids, peptides, amino acids, and their respective derivatives and additional functional groups (see Discussion).

A hierarchical cluster analysis (Fig. 1d) correlates and profiles sorghum genotypes and their respective treatments by their detected compound similarities. The MS treatment is organised under one tree cluster (blue, right), individualised by the respective genotypes SC283-14E (light grey), SC648-14E (grey) and BTx623 (dark grey). Similarly, RP falls within its own tree cluster (red, right), although the SC283-14E and BTx623 branches slightly delineate and include one repetition anomaly found in a different tree. SC648-14E and BTx623 genotypes in the Haz treatment fall into the same tree cluster (red, left), and SC283-14E into another tree (3 of 4 replicates, blue, left). The control nutrient (Control N, left, red) and water (Control W, left, blue) treatments were found between tree clusters.

Genotype-specific exudomes

The van Krevelen diagram for genotype SC283-14E (Fig. 3a) shows the sporadic presence of CHOS compounds with ratios between 1.5 and 1.6 H/C (likely sulphonated polyketides), CHNOS compounds in the ~1.5 H/C

ratio region (terpenoids) and a dominant CHO compound could be annotated as an abscisic acid catabolite (i.e., phaseic acid). The signal intensity for phaseic acid was most prominent for the RP treatment, although still relatively high in the other treatments, comparatively. Notably, the SC648-14E and BTx623 genotypes also produced phaseic acid with the RP treatment (Fig. 3b, c), although only a fraction of the signal strength compared to the SC283-14E genotype.

For genotype SC648-14E (Fig. 3b), two primary compounds were annotated from a cluster of exclusively CHO compounds (likely polyphenols) in the H/C ratio range between 0.6 and 1.0 and on an O/C ratio of 0.3–0.5; these were catechin and 4-O-caffeoylshikimic acid. 4-O-caffeoylshikimic acid is an ester of caffeic acid, belonging to the hydroxycinnamic acid family, and shikimic acid, a cyclohexene-derived acid. The signal intensity of the total compounds detected suggests SC648-14E has a greater exudation profile of CHO compounds compared to SC283-14E and BTx623.

The BTx623 genotype is characterised by its greater presence of CHNO compounds (Fig. 3c). The CHNO compounds are likely represent a diverse mixture of amino acids and/or amino sugars (1.0–2.0 H/C and 0.4–0.8 O/C). The affiliate bar graph shows the signal strength was higher in the No P, RP and SSP treatments, and less so in the Haz and MS treatments.

Exudome responses to hazenite

The van Krevelen diagrams illustrate the differentiating compounds in exudomes of SC283-14E, SC648-14E and BTx623 (Fig. 4a–c) growth with Haz.

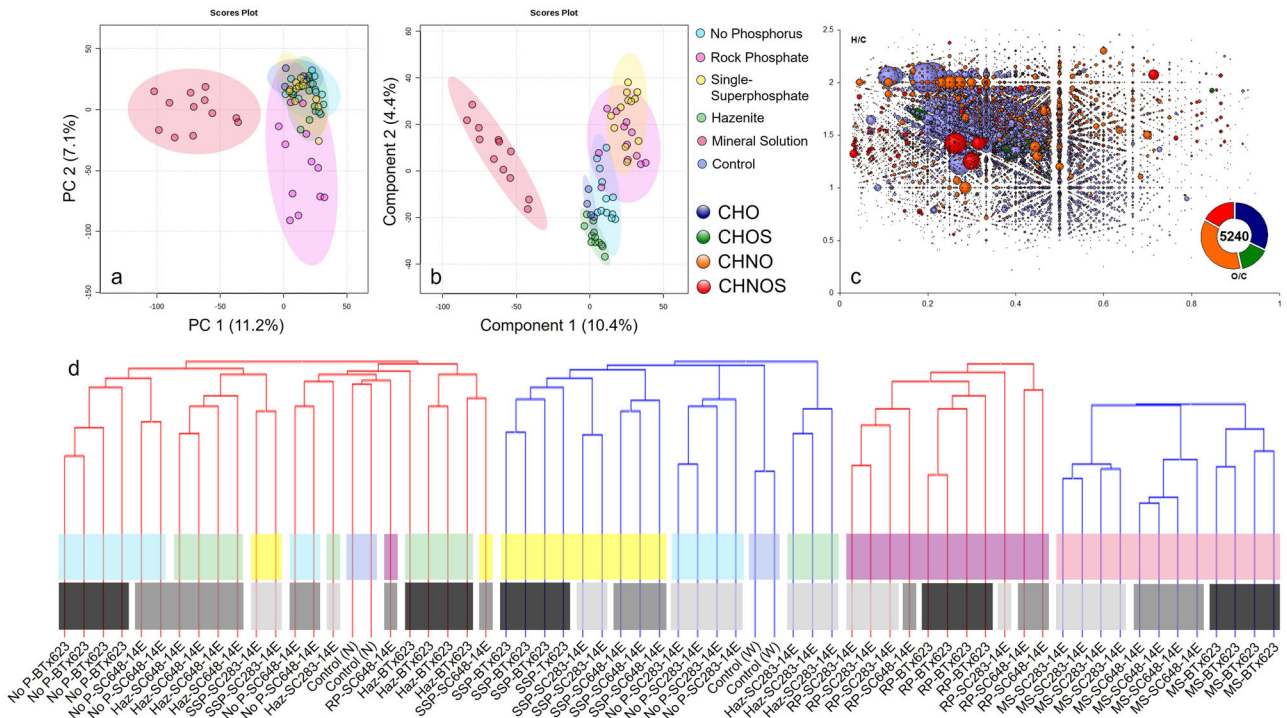


Fig. 2 | Leachate analysis of sorghum root exudation profiles using FT-ICR-MS. Exudome analysis of sorghum genotypes SC283-14E, SC648-14E and BTx623 with different P treatments: principle component analysis (a) and partial least squares discriminant analysis (b) with score plots illustrating the distribution of compounds between P treatments (dot = sample), c van Krevlen diagram depicting the distribution of all detected compounds (H/C versus O/C) from an FT-ICR-MS analysis; the size of the bubbles indicates the signal intensity, the colours represent different molecular

compositions (blue = CHO, green = CHOS, orange = CHNO, and red CHNOS), and the donut chart represents the total and distribution of the compounds, and d hierarchal cluster analysis: the red and blue bars represent grouping and the similarities between exudate clusters; the top coloured rectangle overlaying the red and blue bars match the same colour scheme and treatment profile of the panels 'a' and 'b' (see colour key for treatment details); the bottom rectangles represent the different genotypes and include light grey = SC283-14E, grey = SC648-14E, and dark grey = BTx623.

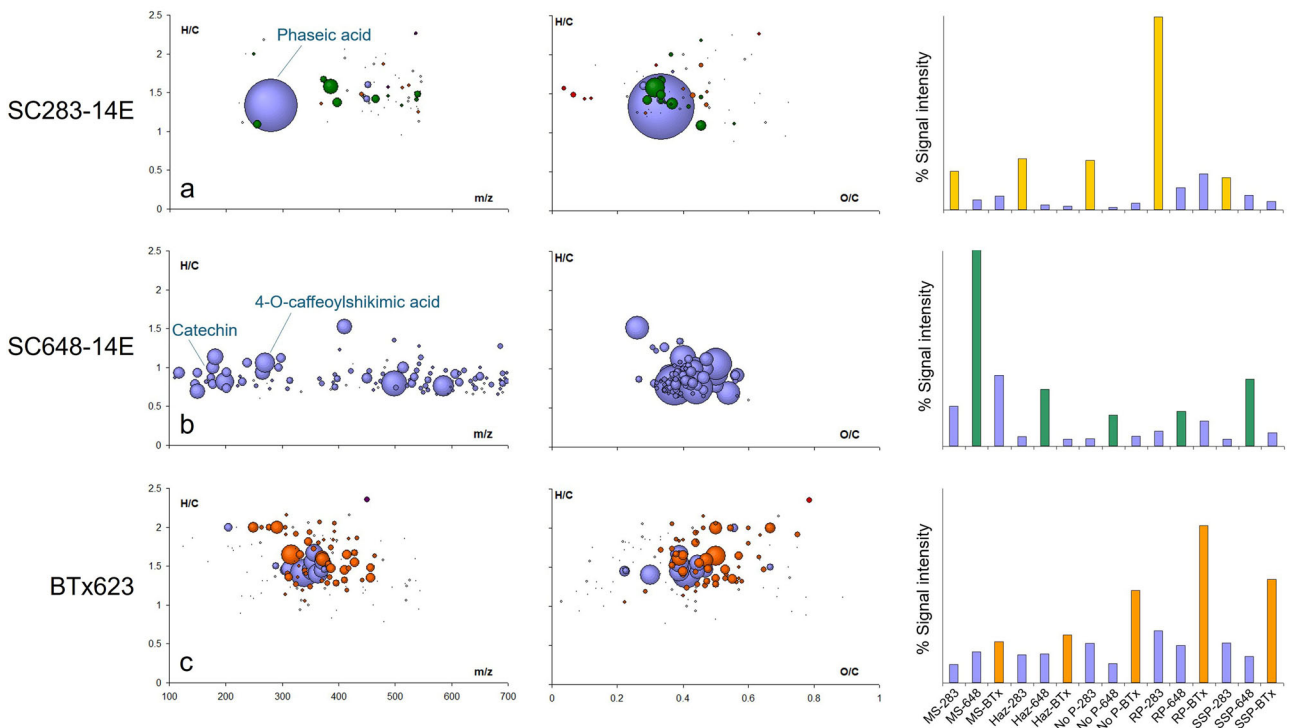


Fig. 3 | Van Krevlen diagrams depicting the distribution of defining detected compounds (H/C versus m/z, and H/C versus O/C). The size of the bubbles indicates the signal intensity, the colours represent different molecular compositions (blue = CHO, green = CHOS, orange = CHNO, and red CHNOS), and the bar

graphs illustrate the signal intensity of the defining detected compounds respective to other treatments. a SC283-14E, bar graph = phaseic acid only, b SC648-14E, bar graph = all detected compounds, and c BTx623, bar graph = all detected compounds.

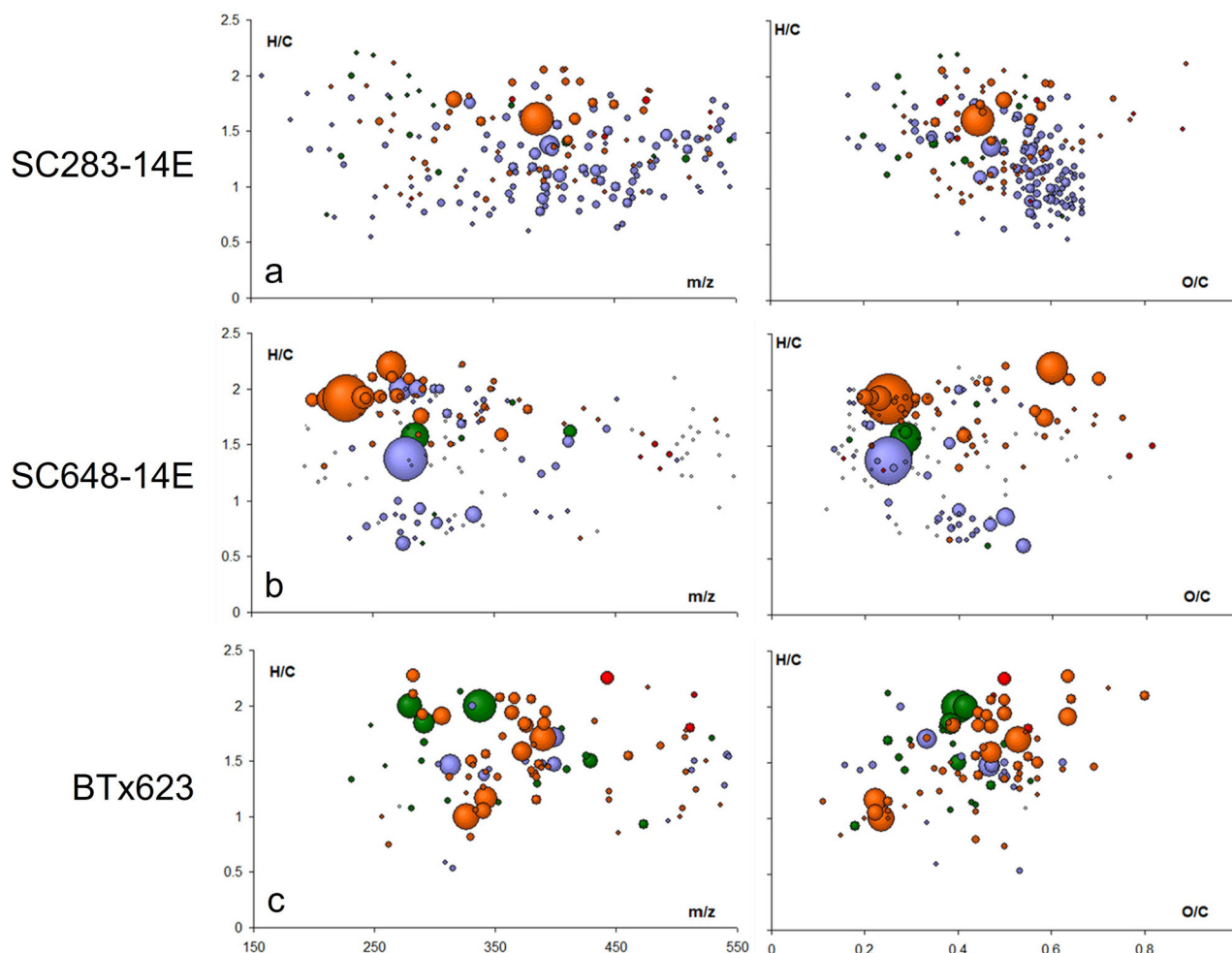


Fig. 4 | Van Krevelen diagrams depicting the distribution of defining detected compounds (H/C versus m/z , and H/C versus O/C) grown with Haz. Three sorghum genotypes are shown: a SC283-14E, b SC648-14E, and c BTx623. Size of the

bubbles indicates the signal intensity, colours represent different molecular compositions (blue = CHO, green = CHOS, orange = CHNO, and red CHNOS). Data extraction profile search at 0.85 threshold.

SC283-14E showed a relatively uniform but wide distribution of CHO and CHON compounds (Fig. 4a). For the CHO family, the H/C ratios ranging from 0.8 to 1.8, strict O/C ratio ending at 0.7, and m/z primarily ranging from 350 to 550, are likely a mixture of flavonoid dimers, tannins, phenolic acid dimers and/or their respective derivatives.

In contrast, SC648-14E shows a distinct shift towards lower m/z values (200–300, Fig. 4b). The broader O/C range suggests enhanced oxidation or oxygen-rich metabolite profiles, possibly including carboxylate or esterified species compared to SC283-14E. In accordance with the H/C and O/C ratios (0.5–1.5 and 0.4–0.6, respectively), the CHO cluster is likely a mixture of phenolic dimers and/or flavonoids. The CHNO compounds are likely N-containing species such as amide and/or peptide derivatives (some of which may represent conjugates or dimers).

BTx623 has a metabolic profile that is distinguished by a broader range of compound families, including CHOS and CHONS compounds. The CHONS family suggests a robust presence of sulphur and nitrogen conjugates, potentially indicating the presence of sulfonated peptides or amino acids, including a more complex metabolite profile involving multifunctionalised compounds and conjugates as discussed below.

Discussion

Total biomass, biomass allocation to roots and shoots, P accumulation and root exudomes confirm that the sorghum genotypes respond differently to P sources and provide evidence for our hypothesis that landraces are more P efficient than an inbred line. SC283-14E had growth

and P accumulation traits that distinguished it from BTx623, and SC648-14E had an intermediate position. We could tentatively confirm the previous assessment of SC283-14E with a large root surface area conveying PUE, as this genotype exceeded the root weight of the other genotypes in some treatments. Perhaps unsurprising, SC648-14E had an intermediate performance because mycorrhizas conveying PUE were excluded from the experiment. Promisingly, root exudomes differed between all genotypes, including between the two landraces that have the Kafir genetic background.

Plants sense P availability and adjust root architecture³⁶. In crops, including sorghum, root length and P uptake can be correlated³⁷. A quantitative trait loci study analysing root architecture alleles found 58% of the enhanced PUE for genotype SC283-14E was due to its enlarged root surface area²⁸. In the studied conditions, all sorghum genotypes had similar root length and root P concentrations. However, SC283-14E had higher root biomass in the RP, SSP and MS treatments than BTx623, which can be caused by greater root diameter, more lateral root branching, and more or longer root hairs to enhance uptake of P and other nutrients³⁸. Higher root biomass without an increase in root length might indicate that the plant is allocating more resources to lateral root growth and/or increasing its root branching rather than expanding it further, which is a strategy to optimise P acquisition^{36,39}. Interestingly, significant differences in root biomass and P concentrations manifested in the least and most bioavailable P treatments (RP and MS, respectively) when comparing SC283-14E and BTx623, supporting the notion that traits of commercial crops differ from landraces,

having been selected in higher P environments typical of high-input agriculture.

SC283-14E exhibited significantly higher total P concentrations in the MS treatment, indicating a superior capacity for P accumulation compared to SC648-14E and BTx623 when provided with soluble P (but did not result in greater biomass production, except when compared to BTx623 in the SSP treatment). On the other hand, SC648-14E produced significantly more biomass in the MS treatment than BTx623, suggesting that SC648-14E may possess enhanced internal PUE. The significantly higher shoot biomass of this genotype, coupled with similar total P content in the no P treatment, further supports the notion of greater internal PUE. Together, these results underscore the different PUE traits of the studied genotypes, including external and internal PUE.

The analysis of compounds in background controls (i.e., microcosms without plants and water only, without plant with nutrient and water) annotated 2100 compounds (Supplementary Fig. 1) that the PCA nested with the No P, SSP and Haz treatments, and centred within the hierarchical tree clusters. A greater number of compounds was detected in all other treatments (No P: 3400 compounds; RP: 3800 compounds; SSP: 3850 compounds; Haz: 2400 compounds), while the MS treatments had 1600 compounds. Thus, up to 1262 ± 582 detected compounds differentiate sorghum genotypes and their respective responses to P treatments. The number of detected compounds detected in our study matches previous research analysing exudates profiles of alfalfa, bean, barley, cucumber, ryegrass, maize, pumpkin and wheat using similar FT-ICR-MS parameters^{6,40}. Lv et al.⁴⁰ used FT-ICR-MS to compare rhizosphere and bulk soil samples and found a similar number of unique detected compounds but almost double the quantity of shared compounds (i.e., detected in both rhizosphere and bulk soil), suggesting microbes produce a similar quantity and compound profiles to maize, cucumber and ryegrass.

The PCA showed RP treatments clustering largely independent from the other treatments, with greater variation of plant responses denoted by the large confidence ellipses, and relatively heterogeneous clustering. This suggests that RP activates a distinct and diverse response between sorghum genotypes. The overlap between No P and RP treatments may suggest similar plant responses with low bioavailability of RP, consistent with the significantly lower biomass and P content compared to all other treatments. This notion is supported by the low solubility and poor bioavailability of RP^{17,41}. Both SSP and Haz treatments had less variability, which indicates closer similarities in detected compounds, possibly due to similar bioavailability with water, citrate and other carboxylates¹².

The MS treatment had the lowest number of detected compounds and differed from other treatments in our analyses (PCA, PLS-DA, hierarchical tree clustering), indicating that plants had a unique response to the non-limiting supply of soluble P. This difference between MS and all other treatments may be explained by (i) plants exuding fewer compounds and/or at lower rates when adequately supplied with P as opposed to exuding compounds that may mobilise P and/or as a nutrient stress response, (ii) MS-supplied plants producing P-containing compounds which were not detected in our analysis, or (iii) RP, SSP, or Haz having chemical constituents that were detected in the analysis.

PLS-DA detected similarities between compounds specific to RP and SSP treatments, which may be explained by both substrates having different bioavailability, but also similarities with constituent elements such as calcium present in considerable quantities in both treatments (~37% and 20% Ca in RP and SSP, respectively)⁴². Other elements are specific to particular P sources, e.g., sulphur with 10% of SSP. Additional sulphur in the SSP and RP treatments may have increased S compound families detected within the SSP treatment and/or altered the plant's exudation profiles in response to these secondary compounds.

Although previous research has characterised sorghum exudates and exudation profiles (Table 1), these studies did not cover the large range of biogeochemical compounds detected in our analysis. Therefore, we have broadened the search to exudates detected in other crops to identify key compounds and their potential function for P mobilisation. The

compounds and their families annotated highlight the primary differences between genotypes and their responses to P treatments. These elemental families are a mixture of metabolites denoted by their elemental structures, some of which likely represent P acquisition mechanisms either directly liberation P from soil or indirectly through microbial relationships.

SC283-14E had phaseic acid (i.e., oxidised abscisic acid) as a dominant compound (Fig. 3). Abscisic acid in its carboxylate form increased P uptake in rice⁴³, wheat and barley⁴⁴. Phaseic acid also has been correlated with mitigating abiotic stressors, including drought in sunflower⁴⁵ and heat in mandarin plants⁴⁶. In the Haz treatment, SC283-14E (Fig. 4) showed conjugates of aromatic carbons and/or organic acids with benzoic acid and tartaric acid as possible compounds. Benzoic acid altered the community composition of soil bacteria⁴⁷ and fungi^{48,49}. Conifers upregulated exudation of tartaric acid under low P supply⁵⁰, and tartaric acid correlates with increased microbial stimulation and root colonisation⁵¹. Thus, these compounds are candidates for P mobilisation, either directly or by stimulating soil microbes possibly adapted for acidic soils with low native soil P seen across Tanzania^{52,53}. With SC283-14E categorised as PUE and showing the highest PUE of the tested genotypes, the next step of research could involve genome and transcriptome analysis to explore to what extent the acids annotated here contribute to PUE.

PUE of SC648-14E has been defined by its relationship with arbuscular mycorrhizal fungi, which correlates with enhanced P uptake under low P conditions²⁹. This genotype had a uniform profile composed of flavonoids and/or polyphenols. Catechin, a flavonoid and polyphenol, can act as an allelochemical antimicrobial agent, a chelating compound supporting P liberation, and has autoinhibitory properties⁵⁴. Inderjit et al.⁵⁵ showed that catechin lowered the presence of microbial communities and reduced plant growth, illustrating its conditional effects. Possible polyphenols include 4-O-caffeoylshikimate (i.e., esterified chlorogenic acid), which increased in tomato exudates of plants inoculated with arbuscular mycorrhizal fungi⁵⁶. Similarly, polyphenol coumaric acid was upregulated in the presence of arbuscular mycorrhizal fungi, which improved P uptake of maize⁵⁷, and boosted some fungi and bacteria communities while inhibiting others⁵⁸. Another detected putative polyphenol, caffeic acid, can serve as an inhibitor of bacteria⁵⁹ and also mitigate abiotic stresses⁶⁰.

A primary candidate for the largest CHO compound detected in the SC648-14E and Haz treatment may be a ferulic acid derivative. When ferulic acid undergoes conjugation or esterification, it can form various derivatives depending on the nature of the conjugation. Ferulic acid is a hydroxycinnamic acid exuded by roots with a wide range of allelopathic functions, including affecting fungi concentrations^{24,61}, lowering bacterial diversity in cucumber⁶², and mitigating fungi disease in tobacco plants⁶³. Thus, the detected flavonoids and polyphenols, including ferulic acid derivatives, may contribute to PUE *via* various means.

There was notable clustering of the CHON family with high saturation and low m/z ratios. These compounds likely reflect peptides or conjugated amino acids with hydroxyl or carboxyl groups and/or moderately saturated alkaloids with possible esterification or functional group attachments. These compounds represent a large option of potential candidates (Table 2), especially considering the extensive range of peptides, amino acids and their respective conjugates and derivatives. Potential compounds include leucylproline (i.e., leucyl, the free radical of leucine) and glutamine. Leucine occurs in higher concentrations in plants under P stress⁴³ and can increase bacteria root colonisation⁶⁴. Leucine and glutamine were produced in greater amounts by arbuscular mycorrhizal fungi in low P conditions⁶⁵, and glutamine has been correlated with improved P and nutrient uptake⁶⁶⁻⁶⁸. Thus, there is evidence that the compounds annotated as characterising SC648-14E are involved in P mobilisation, including interactions with mycorrhizal fungi (which were not studied here).

The BTx623 genotype was largely differentiated from the other genotypes by a mixture of CHO (likely polyketides) and CHON (likely amino acids) elemental families across all P treatments, and notable CHOS and CHONS families in the Haz treatment. Within the Haz treatment, the high H/C ratios suggest the CHOS compounds are sulphur-containing fatty acid

Table 1 | Compilation of known sorghum exudates and their putative effects

Compound name	Formula	Compound associated with	Ubiquitous	Sorghum species	Sorghum bicolor	Reference
CHO elemental family						
5-deoxystrigol	C ₁₉ H ₂₂ O ₅	Germination, N and P deficiency		Y	Y	Awad et al. ⁷⁴ , Yoneyama et al. ²⁵
5-ethoxysorgoleone	C ₂₃ H ₃₁ O ₄	Allelopathy		Y	Y	Czarnota et al. ⁷⁵
alpha-ketoglutaric acid	C ₅ H ₆ O ₅	unspecified	Y			Vranova et al. ³⁵
Arabinose	C ₅ H ₁₀ O ₅	Rhizosphere stimulation	Y	Y	Y	Bertin et al. ⁷⁶ , Vranova et al. ³⁵
Benzoquinone sorgoleone	C ₂₂ H ₃₀ O ₄	Allelopathy		Y	Y	Baerson et al. ⁷⁷
Caffeic acid	C ₉ H ₈ O ₄	Allelopathy			Y	Sène et al. ²²
Citric acid	C ₆ H ₈ O ₇	Iron and P acquisition	Y			Bertin et al. ⁷⁶ , Abadía et al. ⁷⁸ , Bradley and Sieling ⁷⁹
Ferulic acid	C ₁₀ H ₁₀ O ₄	Allelopathy			Y	Sène et al. ²² , Cheema et al. ⁸⁰
Fructose	C ₆ H ₁₂ O ₆	Rhizosphere stimulation	Y	Y	Y	Bertin et al. ⁷⁶ , Vranova et al. ³⁵
Fucose	C ₆ H ₁₂ O ₆	Rhizosphere stimulation	Y			Bertin et al. ⁷⁶
Galactose	C ₆ H ₁₂ O ₆	Rhizosphere stimulation	Y	Y	Y	Bertin et al. ⁷⁶ , Vranova et al. ³⁵
Gallic acid	C ₇ H ₆ O ₅	Allelopathy			Y	Cheema et al. ⁸⁰
Gentisic acid	C ₇ H ₆ O ₅	Allelopathy			Y	Sène et al. ²²
Gluconate	C ₆ H ₁₂ O ₇	Not specified	Y			Vranova et al. ³⁵
Glucose	C ₆ H ₁₂ O ₆	Rhizosphere stimulation	Y	Y	Y	Vranova et al. ³⁵ , Bradley and Sieling ⁷⁹
Glutaric	C ₅ H ₈ O ₄	Nutrient acquisition	Y			Bertin et al. ⁷⁶
Inositol	C ₆ H ₁₂ O ₆	Not specified	Y	Y	Y	Vranova et al. ³⁵
Malic acid	C ₄ H ₆ O ₅	Iron and P acquisition	Y	Y	Y	Bertin et al. ⁷⁶ , Abadía et al. ⁷⁸ , Bradley and Sieling ⁷⁹ , Vranova et al. ³⁵
Maltose	C ₁₂ H ₂₂ O ₁₂	Rhizosphere stimulation	Y			Bertin et al. ⁷⁶
p-coumaric acid	C ₉ H ₈ O ₃	Allelopathy			Y	Sène et al. ²² , Cheema et al. ⁸⁰
p-hydroxybenzoic acid	C ₇ H ₆ O ₃	Allelopathy			Y	Sène et al. ²² , Cheema et al. ⁸⁰
Protocatechuic acid	C ₇ H ₆ O ₄	Allelopathy			Y	Sène et al. ²² , Cheema et al. ⁸⁰ , Kakar et al. ⁸¹
Raffinose	C ₁₈ H ₃₂ O ₁₈	Rhizosphere stimulation	Y			Bertin et al. ⁷⁶
Rhamnose	C ₆ H ₁₂ O ₆	Rhizosphere stimulation	Y			Bertin et al. ⁷⁶
Ribitol	C ₅ H ₁₂ O ₅	Not specified	Y	Y	Y	Vranova et al. ³⁵
Ribose	C ₅ H ₁₀ O ₅	Rhizosphere stimulation	Y			Bertin et al. ⁷⁶
Sorghumol	C ₃₀ H ₅₀ O	Germination stimulant			Y	Awad et al. ⁷⁴
Strigol	C ₁₉ H ₂₂ O ₆	Germination stimulant			Y	Awad et al. ⁷⁴
Sucrose	C ₅ H ₁₀ O ₅	Rhizosphere stimulation	Y	Y	Y	Bertin et al. ⁷⁶ , Vranova et al. ³⁵
Syngaldehyde	C ₉ H ₁₀ O ₄	Allelopathy			Y	Sène et al. ²²
Syringic acid	C ₉ H ₁₀ O ₅	Allelopathy			Y	Sène et al. ²² , Cheema et al. ⁸⁰
Tartaric acid	C ₄ H ₆ O ₆	Nutrient acquisition	Y	Y	Y	Bertin et al. ⁷⁶ , Vranova et al. ³⁵
Tartrate	C ₄ H ₄ O ₆	Phosphorus acquisition	Y			Bradley and Sieling ⁷⁹
Trans-aconitic acid	C ₆ H ₆ O ₆	unspecified	Y	Y	Y	Vranova et al. ³⁵
Vanillic acid	C ₈ H ₈ O ₄	Allelopathy			Y	Sène et al. ²² , Cheema et al. ⁸⁰
Vanillin	C ₈ H ₈ O ₃	Allelopathy			Y	Sène et al. ²²
Xylose	C ₆ H ₁₂ O ₆	unspecified	Y	Y	Y	Bertin et al. ⁷⁶ , Vranova et al. ³⁵
CHON family						
Glutamic acid	C ₅ H ₉ NO ₄	unspecified	Y			Vranova et al. ³⁵
Aspartic acid	C ₄ H ₇ NO ₄	unspecified	Y			Vranova et al. ³⁵
Iso- and -leucine	C ₆ H ₁₃ NO ₂	unspecified	Y	Y	Y	Vranova et al. ³⁵
Lysine	C ₆ H ₁₄ O ₂ N ₂	unspecified	Y	Y	Y	Vranova et al. ³⁵
Arginine	C ₆ H ₁₄ O ₂ N ₄	unspecified	Y	Y	Y	Vranova et al. ³⁵
Histidine	C ₆ H ₉ O ₂ N ₃	unspecified	Y	Y	Y	Vranova et al. ³⁵

Rhizosphere stimulation denotes increased microbial activity.

Table 2 | Analysis of different elemental families and specific compounds not previously characterised in sorghum

Genotype	Hypothesised compound	Formula	m/z	H/C	O/C	Compound function	Reference
CHO elemental family							
SC283-14E	Abscisic acid ^o	C ₁₅ H ₂₀ O ₅	280.12	0.33	1.33	Bacteria stimulation Abiotic regulation	Lopes et al. ⁸² Yang et al. ⁸³ , Zandalinas et al. ⁸³
SC283-14E	Benzoic acid ^c	C ₁₄ H ₁₄ O ₉	372	0.67	0.54	Microbial stimulation/ inhibitor	Liu et al. ⁴⁷ , Liu et al. ⁴⁸ , Windisch et al. ⁴⁸
SC283-14E	Esculin	C ₁₅ H ₁₆ O ₉	340	≈1.0	≈0.6	Iron mobilisation	Schmid et al. ⁸⁴
SC283-14E	Sinapic acid ^d	C ₂₂ H ₂₀ O ₁₀	546	0.73	0.55	Microbial composition	Badri et al. ⁸⁵
SC283-14E	Tartaric acid ^c	C ₁₄ H ₂₂ O ₈	390	1.0	0.6	Bacteria stimulation Phosphorus acquisition Abiotic regulation	Zhang et al. ⁵¹ Yu et al. ⁵⁰ , Wu et al. ⁸⁶ Liu et al. ⁸⁷
SC648-14E	4-O-Caffeoylshikimic acid	C ₁₅ H ₁₄ O ₆	352.08	1.00	0.56	Fungi relationship	Modafar et al. ⁸⁸ , Ziouti et al. ⁸⁹
SC648-14E	Caffeic acid ^d	C ₁₈ H ₁₆ O ₈	516	0.75	0.58	Abiotic regulation Bacteria inhibitor	Mughal et al. ⁶⁰ Li et al. ⁵⁹
SC648-14E	Catechin	C ₁₅ H ₁₄ O ₆	290.27	≈0.933	0.4	Phosphorus + fungi symbiosis Phytotoxin, allelochemical	Zabinski et al. ⁹⁰ Perry et al. ⁵⁴
SC648-14E	Citric acid	C ₆ H ₈ O ₇	192.12	≈1.33	≈1.17	Phosphorus acquisition	Neumann and Römheld ⁹¹
SC648-14E	Coumaric acid ^d	C ₁₈ H ₁₆ O ₈	516	0.75	0.58	Microbial stimulation/ inhibitor Root-fungi relationship	Zhou and Wu ⁵⁸ Ma et al. ⁵⁷
SC648-14E	Ferulic acid ^{e/z}	≈C ₁₀ H ₁₀ O ₄	≈275	1.0–1.5	0.25–0.4	Fungi stimulation	Zhou and Wu ⁶² , Rahman et al., ²⁴ Jin et al. ⁵¹
SC648-14E	Gallic Acid ^d	C ₁₄ H ₁₀ O ₁₀	338.24	≈0.714	≈0.714	Microbial respiration Bacteria chemoattractant	Davies et al. ⁹² Ray et al. ⁹³
SC648-14E	Protocatechuic acid ^d	C ₁₄ H ₁₀ O ₇	306.24	≈0.714	0.5	Root-fungi relationship P acquisition	Ma et al. ⁵⁷ Luo et al. ⁹⁴
SC648-14E	Salicylic acid ^d	C ₁₄ H ₁₂ O ₆	276.24	≈0.857	≈0.429	Fungi stimulation	Clocchiatti et al. ⁹⁵
CHON elemental family							
SC648-14E	Glutamine ^{e/e}	C ₅ H ₁₀ N ₂ O ₃	≈250–300	≈2	≈0.3–0.4	Nutrient acquisition Phosphorus acquisition	Tawaraya et al. ⁶⁸ De Andrade et al., Edayilam et al. ^{66,67}
SC648-14E	Leucyl-proline ^z	≈C ₁₁ H ₂₀ N ₂ O ₃	≈288	1.82	0.27	Leucyl: Fungi stimulation Leucyl: Phosphorus acquisition Proline: abiotic regulation	Liu et al. ⁹⁶ Tawaraya et al. ⁴³ Vives-Peris et al. ⁹⁷
SC648-14E	Nicotianamine ^z	≈C ₁₂ H ₂₄ N ₃ O ₆	≈310	≈2.0	≈0.5	Nutrient acquisition	Chen et al. ⁹⁸ , Tsednee et al. ^{98,99}
SC648-14E	Phenylalanine ^{e/e}	C ₉ H ₁₁ NO ₂	≈175–300	≈1.83	≈0.22–0.3	Root signalling Fungi stimulation/inhibition Abiotic regulation	Yu et al. ¹⁰⁰ Liu et al. ⁹⁶ Sulochana ¹⁰¹
SC648-14E	Scopolamine	C ₁₇ H ₂₃ NO ₃	≈303	≈1.88	≈0.35–0.4	Bacteria relationship	Jousse et al. ¹⁰²
SC648-14E	Stearic acid ^{a/e/o}	C ₁₈ H ₃₅ NO ₂	≈285	≈1.95	≈0.1–0.2	Microbial stimulation/ inhibition	Ankati et al. ¹⁰³ , Mungur et al. ¹⁰⁴
CHONS elemental family							
BTx623	Cysteine	C ₃ H ₇ NO ₂ S	≈0.67	≈2.33	121.16	Phosphorus acquisition Bacteria relationship	Wu et al. ⁸⁶ Mavrodi et al. ⁶⁹
BTx623	Methionine	C ₅ H ₁₁ NO ₂ S	0.4	2.2	149.21	Microbial stimulation/ inhibition	Liu et al. ⁹⁶ , Liang et al. ¹⁰⁵

Potential compounds derived by their mass to charge ratio (m/z), hydrogen to carbon ratio (H/C) and oxygen to carbon ratio (O/C). The hypothesised compounds and their respective derivatives denoted by superscript letters and include amide (a), conjugate (c), dimer (d), esters (e), oxygenated (o) and other/multiple derivative(s) (z).

derivatives or thioesters with long alkyl chains and an attached functional group. Similarly, the detected CHONS compounds may be complex conjugates involving a sulphur-containing amino acid (such as cysteine or methionine) with an added functional group or conjugate. Cysteine and methionine are exuded by roots to provide sulphur to microbes⁶⁹, and are compounds for unidirectional root-microbial nutrient cycling of nitrogen and sulphur^{70,71}. Under non-limiting hydroponic conditions, BTx623 exuded higher concentrations of mono- and di-saccharides when compared to other sorghum varieties, which promoted a distinct microbial community composition⁷². While these sugars were not prominent in our analysis,

Miller et al.⁷³ demonstrated that soil type influences exudation profiles annotated as rhizosphere-conditioners and microbial recruitment compounds. This may suggest BTx623 exudation profiles are oriented toward rhizosphere conditioning and microbial interactions over direct P mobilisation.

Taken together, our study presents evidence that the sorghum genotypes have different exudate profiles. Many of these compounds have previously been annotated and are involved in plant-microbe interactions, nutrient mobilisation including P mobilisation, and exuded in response to stress. Subsequent research can build on these findings, connecting to crop

breeders' tools and evaluate contrasting sorghum lines in controlled and real-world environments to deepen causal understanding and harness root exudates for direct and indirect P mobilisation.

This study demonstrated that non-target root exudome analysis can identify distinct compounds produced by sorghum genotypes, illustrating that specific compounds may reflect each genotype's unique adaptations to low P environments and contribute to P mobilisation, beneficial microbial relationships and stress mitigation. Greater biomass and/or P uptake of landraces compared to the inbred line studied here confirms that landraces have superior PUE, which is likely the result of having been selected in low P environments. Thus, there is an opportunity to enhance PUE through the selection of genotypes paired with P sources, including less soluble recycles that are becoming available as nations transition from the current linear to a circular phosphorus economy. Hazenite emerges as an effective P source and candidate to substitute superphosphate fertiliser. Integrating powerful 'omics approaches has much potential to advance PUE of crops and enable P-efficient cropping and the next-generation fertilisers generated in the circular P economy.

Data availability

The datasets generated and/or analysed during the current study are not publicly available because they were generated using custom analytical code developed by our laboratory over an extended period and are not currently publicly released, but are available from the corresponding author on reasonable request.

Received: 19 August 2025; Accepted: 19 January 2026;

Published online: 31 March 2026

References

- Marschner, P. & Rengel, Z. in *Marschner's Mineral Nutrition of Plants 4th Edn* (eds Rengel Z., Cakmak I. & White P. J.) 499–522 (Academic Press, 2023).
- Pantigoso, H. A., Manter, D. K., Fonte, S. J. & Vivanco, J. M. Root exudate-derived compounds stimulate the phosphorus solubilizing ability of bacteria. *Sci. Rep.* **13**, 4050 (2023).
- Preece, C. & Peñuelas, J. A return to the wild: root exudates and food security. *Trends Plant Sci.* **25**, 14–21 (2020).
- Jha, U. C. et al. Breeding and genomics approaches for improving phosphorus-use efficiency in grain legumes. *Environ. Exp. Bot.* **205**, 105120 (2023).
- Vives-Peris, V., de Ollas, C., Gómez-Cadenas, A. & Pérez-Clemente, R. M. Root exudates: from plant to rhizosphere and beyond. *Plant Cell Rep.* **39**, 3–17 (2020).
- Miao, Y., Lv, J., Huang, H., Cao, D. & Zhang, S. Molecular characterization of root exudates using Fourier transform ion cyclotron resonance mass spectrometry. *J. Environ. Sci.* **98**, 22–30 (2020).
- Escolà Casas, M. & Matamoros, V. Analytical challenges and solutions for performing metabolomic analysis of root exudates. *Trends Environ. Anal. Chem.* **31**, e00130 (2021).
- Walsh, M., Schenk, G. & Schmidt, S. Realising the circular phosphorus economy delivers for sustainable development goals. *npj Sustain. Agric.* **1**, 2 (2023).
- Watson, C., Clemens, J. & Wichern, F. Hazenite: a new secondary phosphorus, potassium and magnesium fertiliser. *Plant, Soil Environ.* **66**, 1–6 (2020).
- Raniro, H. R., Teles, A. P. B., Adam, C. & Pavinato, P. S. Phosphorus solubility and dynamics in a tropical soil under sources derived from wastewater and sewage sludge. *J. Environ. Manag.* **302**, 113984 (2022).
- Zhao, S. et al. A precision compost strategy aligning composts and application methods with target crops and growth environments can increase global food production. *Nat. Food* **3**, 741–752 (2022).
- Walsh, M. et al. The circular phosphorus economy: agronomic performance of recycled fertilizers and target crops. *J. Plant Nutr. Soil Sci.* <https://doi.org/10.1002/jpln.202400299> (2025).
- Dissanayaka, D. M. S. B., Ghahremani, M., Siebers, M., Wasaki, J. & Plaxton, W. C. Recent insights into the metabolic adaptations of phosphorus-deprived plants. *J. Exp. Bot.* **72**, 199–223 (2020).
- Han, Y., White, P. J. & Cheng, L. Mechanisms for improving phosphorus utilization efficiency in plants. *Ann. Bot.* **129**, 247–258 (2022).
- Lambers, H. Phosphorus acquisition and utilization in plants. *Annu. Rev. Plant Biol.* **73**, 17–42 (2022).
- Feder, D. et al. Structural elements that modulate the substrate specificity of plant purple acid phosphatases: avenues for improved phosphorus acquisition in crops. *Plant Sci.* **294**, 110445 (2020).
- Bolland, M., Gilkes, R. & Antuono, M. The effectiveness of rock phosphate fertilisers in Australian agriculture: a review. *Aust. J. Exp. Agric.* **28**, 655–668 (1988).
- Hertzberger, A. J., Cusick, R. D. & Margenot, A. J. A review and meta-analysis of the agricultural potential of struvite as a phosphorus fertilizer. *Soil Sci. Soc. Am. J.* **84**, 653–671 (2020).
- Hauck, D., Lohr, D., Meinken, E. & Schmidhalter, U. Availability of phosphorus recovered from waste streams to plants cultivated in soilless growing media. *J. Plant Nutr. Soil Sci.* **184**, 733–744 (2021).
- Bakari, H. et al. Sorghum (*Sorghum bicolor* L. Moench) and its main parts (By-Products) as promising sustainable sources of value-added ingredients. *Waste Biomass. Valoriz.* **14**, 1023–1044 (2023).
- Mace, E. S. et al. Whole-genome sequencing reveals untapped genetic potential in Africa's indigenous cereal crop sorghum. *Nat. Commun.* **4**, 2320 (2013).
- Sène, M., Doré, T. & Pellissier, F. Effect of phenolic acids in soil under and between rows of a prior sorghum (*Sorghum bicolor*) crop on germination, emergence, and seedling growth of peanut (*Arachis hypogea*). *J. Chem. Ecol.* **26**, 625–637 (2000).
- Balasubramanian, V. K. et al. Induced secretion system mutation alters rhizosphere bacterial composition in *Sorghum bicolor* (L.) Moench. *Planta* **253**, 33 (2021).
- Jin, X., Wu, F. & Zhou, X. Different toxic effects of ferulic and p-hydroxybenzoic acids on cucumber seedling growth were related to their different influences on rhizosphere microbial composition. *Biol. Fertil. Soils* **56**, 125–136 (2020).
- Yoneyama, K. et al. Nitrogen deficiency as well as phosphorus deficiency in sorghum promotes the production and exudation of 5-deoxystigol, the host recognition signal for arbuscular mycorrhizal fungi and root parasites. *Planta* **227**, 125–132 (2007).
- de Oliveira, I. F. et al. Sorgoleone concentration influences mycorrhizal colonization in sorghum. *Mycorrhiza* **31**, 259–264 (2021).
- Tao, Y. et al. Large-scale GWAS in sorghum reveals common genetic control of grain size among cereals. *Plant Biotechnol. J.* **18**, 1093–1105 (2020).
- Bernardino, K. C. et al. The genetic architecture of phosphorus efficiency in sorghum involves pleiotropic QTL for root morphology and grain yield under low phosphorus availability in the soil. *BMC Plant Biol.* **19**, 87 (2019).
- Watts-Williams, S. J. et al. Enhancement of sorghum grain yield and nutrition: a role for arbuscular mycorrhizal fungi regardless of soil phosphorus availability. *Plants People Planet* **4**, 143–156 (2022).
- Miller, F. Release of A&BTx622, 623, 624. *Report of Technical Committee on Seed Release and Increase* (1977).
- Baloch, F. S. et al. Recent advancements in the breeding of sorghum crop: current status and future strategies for marker-assisted breeding. *Front. Genet.* **14**, 1150616 (2023).
- Lindsey, B. E., Rivero, L., Calhoun, C. S., Grotewold, E. & Brkljacic, J. Standardized method for high-throughput sterilization of *Arabidopsis* seeds. *J. Visual. Exp.* e56587 (2017).
- Wolf, D. C. & Skipper, H. D. in *Methods of Soil Analysis* 41–51 (1994).
- Inselsbacher, E. et al. A cost-effective high-throughput microcosm system for studying nitrogen dynamics at the plant-microbe-soil interface. *Plant Soil* **317**, 293–307 (2009).

35. Vranova, V., Rejsek, K., Skene, K. R., Janous, D. & Formanek, P. Methods of collection of plant root exudates in relation to plant metabolism and purpose: a review. *J. Plant Nutr. Soil Sci.* **176**, 175–199 (2013).
36. Niu, Y. F. et al. Responses of root architecture development to low phosphorus availability: a review. *Ann. Bot.* **112**, 391–408 (2012).
37. Otani, T. & Ae, N. Sensitivity of phosphorus uptake to changes in root length and soil volume. *Agron. J.* **88**, 371–375 (1996).
38. Nibau, C., Gibbs, D. J. & Coates, J. C. Branching out in new directions: the control of root architecture by lateral root formation. *N. Phytol.* **179**, 595–614 (2008).
39. Ryser, P. The mysterious root length. *Plant Soil* **286**, 1–6 (2006).
40. Lv, L. et al. Unique dissolved organic matter molecules and microbial communities in rhizosphere of three typical crop soils and their significant associations based on FT-ICR-MS and high-throughput sequencing analysis. *Sci. Total Environ.* **919**, 170904 (2024).
41. Chien, S. H., Prochnow, L. I., Tu, S. & Snyder, C. S. Agronomic and environmental aspects of phosphate fertilizers varying in source and solubility: an update review. *Nutr. Cycl. Agroecosyst.* **89**, 229–255 (2011).
42. Ryszko, U., Rusek, P. & Kolodyńska, D. Quality of phosphate rocks from various deposits used in wet phosphoric acid and P-fertilizer production. *Materials* **16** <https://doi.org/10.3390/ma16020793> (2023).
43. Tawaraya, K. et al. Metabolite profiling of shoot extracts, root extracts, and root exudates of rice plant under phosphorus deficiency. *J. Plant Nutr.* **36**, 1138–1159 (2013).
44. Nobile, C. et al. Phosphorus-acquisition strategies of canola, wheat and barley in soil amended with sewage sludges. *Sci. Rep.* **9**, 14878 (2019).
45. Bano, A., Hansen, H., Dörffling, K. & Hahn, H. Changes in the contents of free and conjugated abscisic acid, phaseic acid and cytokinins in xylem sap of drought stressed sunflower plants. *Phytochemistry* **37**, 345–347 (1994).
46. Zandalinas, S. I., Rivero, R. M., Martínez, V., Gómez-Cadenas, A. & Arbona, V. Tolerance of citrus plants to the combination of high temperatures and drought is associated to the increase in transpiration modulated by a reduction in abscisic acid levels. *BMC Plant Biol.* **16**, 105 (2016).
47. Liu, Y. et al. Identification of benzoic acid and 3-phenylpropanoic acid in tobacco root exudates and their role in the growth of rhizosphere microorganisms. *Appl. Soil Ecol.* **93**, 78–87 (2015).
48. Liu, J., Li, X., Jia, Z., Zhang, T. & Wang, X. Effect of benzoic acid on soil microbial communities associated with soilborne peanut diseases. *Appl. Soil Ecol.* **110**, 34–42 (2017).
49. Windisch, S. et al. Role of benzoic acid and lettukenin a in the defense response of lettuce against soil-borne pathogens. *Plants* **10**, 2336 (2021).
50. Yu, Y., Yu, J., Shan, Q., Fang, L. & Jiang, D. Organic acid exudation from the roots of *Cunninghamia lanceolata* and *Pinus massoniana* seedlings under low phosphorus stress. *Front. For. China* **3**, 117–120 (2008).
51. Zhang, H. et al. The enhanced mechanisms of Hansschlegelia zihuaiae S113 degrading bensulfuron-methyl in maize rhizosphere by three organic acids in root exudates. *Ecotoxicol. Environ. Saf.* **223**, 112622 (2021).
52. Agegnehu, G. et al. Extent and management of acid soils for sustainable crop production system in the tropical agroecosystems: a review. *Acta Agric. Scand. B Soil Plant Sci.* <https://doi.org/10.1080/09064710.2021.1954239> (2021).
53. Nishigaki, T. et al. Fractionation of phosphorus in soils with different geological and soil physicochemical properties in southern Tanzania. *Soil Sci. Plant Nutr.* **64**, 291–299 (2018).
54. Perry, L. G., Weir, T. L., Prithiviraj, B., Paschke, M. W. & Vivanco, J. M. in *Communication in Plants: Neuronal Aspects of Plant Life* (eds Baluška F., Mancuso S. & Volkmann D.) 403–420 (Springer, 2006).
55. Inderjit, Kaur, R., Kaur, S. & Callaway, R. M. Impact of (±)-catechin on soil microbial communities. *Commun. Integr. Biol.* **2**, 127–129 (2009).
56. Negrel, J., Javelle, F., Morandi, D. & Lucchi, G. Characterization and purification of a bacterial chlorogenic acid esterase detected during the extraction of chlorogenic acid from arbuscular mycorrhizal tomato roots. *Plant Physiol. Biochem.* **109**, 308–318 (2016).
57. Ma, J. et al. Mycorrhizal symbiosis promotes the nutrient content accumulation and affects the root exudates in maize. *BMC Plant Biol.* **22**, 64 (2022).
58. Zhou, X. & Wu, F. p-Coumaric acid influenced cucumber rhizosphere soil microbial communities and the growth of *Fusarium oxysporum* f. sp. *cucumerinum* Owen. *PLoS ONE* **7**, e48288 (2012).
59. Li, S. et al. Caffeic acid in tobacco root exudate defends tobacco plants from infection by *Ralstonia solanacearum*. *Front. Plant Sci.* **12**, 690586 (2021).
60. Mughal, A. et al. Exploring the role of caffeic acid in mitigating abiotic stresses in plants: a review. *Plant Stress* **12**, 100487 (2024).
61. Rahman, U. et al. Exogenously applied ferulic acid and p-coumaric acid differentially affect cucumber rhizosphere *Trichoderma* spp. community structure and abundance. *Plant Soil Environ.* **66**, 461–467 (2020).
62. Zhou, X. & Wu, F. Effects of amendments of ferulic acid on soil microbial communities in the rhizosphere of cucumber (*Cucumis sativus* L.). *Eur. J. Soil Biol.* **50**, 191–197 (2012).
63. Zhang, C., Feng, C., Zheng, Y., Wang, J. & Wang, F. Root exudates metabolic profiling suggests distinct defense mechanisms between resistant and susceptible tobacco cultivars against black shank disease. *Front. Plant Sci.* **11**, 559775 (2020).
64. la Rosa, G. M. -d et al. Amino acids in the root exudates of *Agave lechuguilla* Torr. favor the recruitment and enzymatic activity of nutrient-improvement rhizobacteria. *Microb. Ecol.* **86**, 1176–1188 (2023).
65. Luthfiana, N. et al. Metabolite profiling of the hyphal exudates of *Rhizophagus clarus* and *Rhizophagus irregularis* under phosphorus deficiency. *Mycorrhiza* **31**, 403–412 (2021).
66. Edayilam, N. et al. Phosphorus stress-induced changes in plant root exudation could potentially facilitate uranium mobilization from stable mineral forms. *Environ. Sci. Technol.* **52**, 7652–7662 (2018).
67. Tawaraya, K., Horie, R., Wagatsuma, T., Saito, K. & Oikawa, A. Metabolite profiling of shoot extract, root extract, and root exudate of rice under nitrogen and phosphorus deficiency. *Soil Sci. Plant Nutr.* **64**, 312–322 (2018).
68. De Andrade, S. A. L. et al. Phosphorus shortage induces an increase in root exudation in fifteen eucalypts species. *Agronomy* **12**, 2041 (2022).
69. Mavrodi, O. V. et al. Root exudates alter the expression of diverse metabolic, transport, regulatory, and stress response genes in rhizosphere *Pseudomonas*. *Front. Microbiol.* **12**, 651282 (2021).
70. Wang, D., Wang, J., Chadwick, D. R., Ge, T. & Jones, D. L. Competition for two sulphur containing amino acids (cysteine and methionine) by soil microbes and maize roots in the rhizosphere. *Biol. Fertil. Soils* **59**, 697–704 (2023).
71. Ma, Q., Hill, P. W., Chadwick, D. R., Wu, L. & Jones, D. L. Competition for S-containing amino acids between rhizosphere microorganisms and plant roots: the role of cysteine in plant S acquisition. *Biol. Fertil. Soils* **57**, 825–836 (2021).
72. Seitz, V. A. et al. Variation in root exudate composition influences soil microbiome membership and function. *Appl. Environ. Microbiol.* **88**, e00226–00222 (2022).
73. Miller, S. B., Heuberger, A. L., Broeckling, C. D. & Jahn, C. E. Non-targeted metabolomics reveals sorghum rhizosphere-associated

- exudates are influenced by the belowground interaction of substrate and sorghum genotype. *Int. J. Mol. Sci.* **20**, 431 (2019).
74. Awad, A. A. et al. Characterization of strigolactones, germination stimulants for the root parasitic plants striga and orobanche, produced by maize, millet and sorghum. *Plant Growth Regul.* **48**, 221–227 (2006).
 75. Czarnota, M. A., Rimando, A. M. & Weston, L. A. Evaluation of root exudates of seven sorghum accessions. *J. Chem. Ecol.* **29**, 2073–2083 (2003).
 76. Bertin, C., Yang, X. & Weston, L. A. The role of root exudates and allelochemicals in the rhizosphere. *Plant Soil* **256**, 67–83 (2003).
 77. Baerson, S. R. et al. A functional genomics investigation of allelochemical biosynthesis in Sorghum bicolor root hairs. *J. Biol. Chem.* **283**, 3231–3247 (2008).
 78. Abadía, J., López-Millán, A.-F., Rombolà, A. & Abadía, A. Organic acids and Fe deficiency: a review. *Plant Soil* **241**, 75–86 (2002).
 79. Bradley, D. B. & Sieling, D. H. Effect of organic anions and sugars on phosphate precipitation by iron and aluminum as influenced By pH. *Soil Sci.* **76**, 175–180 (1953).
 80. Cheema, Z., Khaliq, A., Abbas, M. & Farooq, M. Allelopathic potential of sorghum (*Sorghum bicolor* L. Moench) cultivars for weed management. *Allelopath. J.* **20**, 167 (2007).
 81. Kakar, K., Xuan, T. D. & Khanh, T. D. Allelopathic potential of sweet sorghum root exudates and identification of the relevant allelochemicals. *Agrochemicals* **2**, 96–105 (2023).
 82. Lopes, L. D., Futrell, S. L., Bergmeyer, E., Hao, J. & Schachtman, D. P. Root exudate concentrations of indole-3-acetic acid (IAA) and abscisic acid (ABA) affect maize rhizobacterial communities at specific developmental stages. *FEMS Microbiol. Ecol.* **99** <https://doi.org/10.1093/femsec/fiad019> (2023).
 83. Yang, J., Zhang, J., Wang, Z., Zhu, Q. & Liu, L. Abscisic acid and cytokinins in the root exudates and leaves and their relationship to senescence and remobilization of carbon reserves in rice subjected to water stress during grain filling. *Planta* **215**, 645–652 (2002).
 84. Schmid, N. B. et al. Feruloyl-CoA 6'-hydroxylase1-dependent coumarins mediate iron acquisition from alkaline substrates in Arabidopsis. *Plant Physiol.* **164**, 160–172 (2013).
 85. Badri, D. V. et al. An ABC transporter mutation alters root exudation of phytochemicals that provoke an overhaul of natural soil microbiota. *Plant Physiol.* **151**, 2006–2017 (2009).
 86. Wu, Y. et al. Multi-omics-based identification of purple acid phosphatases and metabolites involved in phosphorus recycling in stylo root exudates. *Int. J. Biol. Macromol.* **241**, 124569 (2023).
 87. Liu, B., Wu, L., Pan, P., Li, R. & Lin, B. Response of root exudates of *Bruguiera gymnorhiza* (L.) to exposure of polycyclic aromatic hydrocarbons. *Front. Environ. Sci.* **9**, 787002 (2022).
 88. Modafar, C. E., Tantaoui, A. & Boustani, E. Effet de L'acide Caféoylshikimique des Racines du Palmier Dattier sur L'activité et la Production des Enzymes Hydrolytiques de *Fusarium oxysporum* f. sp. *albedinis*. *J. Phytopathol.* **148**, 101–108 (2000).
 89. Ziouti, A., El Modafar, C., Fleuriet, A., El Boustani, S. & Macheix, J. Phenolic compounds in date palm cultivars sensitive and resistant to *Fusarium oxysporum*. *Biol. Plant.* **38**, 451–457 (1996).
 90. Zabinski, C. A., Quinn, L. & Callaway, R. M. Phosphorus uptake, not carbon transfer, explains arbuscular mycorrhizal enhancement of *Centaurea maculosa* in the presence of native grassland species. *Funct. Ecol.* **16**, 758–765 (2002).
 91. Neumann, G. & Römheld, V. Root excretion of carboxylic acids and protons in phosphorus-deficient plants. *Plant Soil* **211**, 121–130 (1999).
 92. Davies, T. K. R., Lovelock, C. E., Pettit, N. E. & Grierson, P. F. Short-term microbial respiration in an arid zone mangrove soil is limited by availability of gallic acid, phosphorus and ammonium. *Soil Biol. Biochem.* **115**, 73–81 (2017).
 93. Ray, S. et al. Modulation in phenolic root exudate profile of *Abelmoschus esculentus* expressing activation of defense pathway. *Microbiol. Res.* **207**, 100–107 (2018).
 94. Luo, J. et al. Metabolic alterations provide insights into *Stylosanthes* roots responding to phosphorus deficiency. *BMC Plant Biol.* **20**, 85 (2020).
 95. Clocchiatti, A., Hannula, S. E., Van den Berg, M., Hundscheid, M. P. & De Boer, W. Evaluation of phenolic root exudates as stimulants of saprotrophic fungi in the rhizosphere. *Front. Microbiol.* **12**, 644046 (2021).
 96. Liu, B., Wu, F., Yang, Y. & Wang, X. Amino acids in watermelon root exudates and their effect on growth of *Fusarium oxysporum* f. sp. *neivium*. *Allelopath. J.* **23**, 139–148 (2009).
 97. Vives-Peris, V., Gómez-Cadenas, A. & Pérez-Clemente, R. M. Citrus plants exude proline and phytohormones under abiotic stress conditions. *Plant Cell Rep.* **36**, 1971–1984 (2017).
 98. Chen, Y.-T., Wang, Y. & Yeh, K.-C. Role of root exudates in metal acquisition and tolerance. *Curr. Opin. Plant Biol.* **39**, 66–72 (2017).
 99. Tsednee, M., Yang, S.-C., Lee, D.-C. & Yeh, K.-C. Root-secreted nicotianamine from *Arabidopsis halleri* facilitates zinc hypertolerance by regulating zinc bioavailability. *Plant Physiol.* **166**, 839–852 (2014).
 100. Yu, H., Gao, D., Khashi u Rahman, M., Chen, S. & Wu, F. L-phenylalanine in potato onion (*Allium cepa* var. *aggregatum* G. Don) root exudates mediates neighbor detection and trigger physio-morphological root responses of tomato. *Front. Plant Sci.* **14**, 1056629 (2023).
 101. Sulochana, M. C. B. Amino acids in root exudates of cotton. *Plant Soil* **16**, 312–326 (1962).
 102. Jousse, C. et al. Tropane alkaloid profiling of hydroponic *Datura innoxia* mill. Plants inoculated with *Agrobacterium rhizogenes*. *Phytochem. Anal.* **21**, 118–127 (2010).
 103. Ankati, S., Rani, T. S. & Podile, A. R. Changes in root exudates and root proteins in groundnut-pseudomonas sp. interaction contribute to root colonization by bacteria and defense response of the host. *J. Plant Growth Regul.* **38**, 523–538 (2019).
 104. Mungur, R., Glass, A. D., Goodenow, D. B. & Lightfoot, D. A. Metabolite fingerprinting in transgenic *Nicotiana tabacum* altered by the *Escherichia coli* glutamate dehydrogenase gene. *J. Biomed. Biotechnol.* **2005**, 198–214 (2005).
 105. Liang, J. et al. Comparison of the rhizosphere bacterial communities of Zigongdongdou soybean and a high-methionine transgenic line of this cultivar. *PLoS ONE* **9**, e103343 (2014).

Acknowledgements

We thank SF-SoepenberGmbH for providing the hazenite. This research was supported by an HDR Scholarship to MW from The University of Queensland and top-up stipend from the End Food Waste Cooperative Research Centre whose activities are funded by the Australian Government's Cooperative Research Centre Program.

Author contributions

Michael Walsh: conceptualisation, methodology, formal analysis, investigation, resources, data curation, writing—original draft, writing—review and editing, visualization, funding acquisition; Philippe Schmitt-Kopplin: methodology, software, validation, formal analysis, investigation, resources, data curation, writing—review and editing, visualization, funding acquisition; Jenny Uhl: formal analysis, validation, writing—review and editing; Marianna Lucio: formal analysis, writing—review and editing; Hector Vera Wood: formal analysis, writing—review and editing; Gerhard Schenk: writing—review and editing, supervision; David Jordan: writing—review and editing; Emma Mace: writing—review and editing; Susanne Schmidt: conceptualisation, methodology, resources, writing—original draft, writing—review and editing, supervision, project administration.

Competing interests

The authors declare no competing interests.

Additional information

Supplementary information The online version contains supplementary material available at

<https://doi.org/10.1038/s44264-026-00134-z>.

Correspondence and requests for materials should be addressed to Susanne Schmidt.

Reprints and permissions information is available at

<http://www.nature.com/reprints>

Publisher's note Springer Nature remains neutral with regard to jurisdictional claims in published maps and institutional affiliations.

Open Access This article is licensed under a Creative Commons Attribution-NonCommercial-NoDerivatives 4.0 International License, which permits any non-commercial use, sharing, distribution and reproduction in any medium or format, as long as you give appropriate credit to the original author(s) and the source, provide a link to the Creative Commons licence, and indicate if you modified the licensed material. You do not have permission under this licence to share adapted material derived from this article or parts of it. The images or other third party material in this article are included in the article's Creative Commons licence, unless indicated otherwise in a credit line to the material. If material is not included in the article's Creative Commons licence and your intended use is not permitted by statutory regulation or exceeds the permitted use, you will need to obtain permission directly from the copyright holder. To view a copy of this licence, visit <http://creativecommons.org/licenses/by-nc-nd/4.0/>.

© The Author(s) 2026